On the Development of Coherent Structure in a Plane Jet*
(Part 2, Investigation of Spatio-Temporal Velocity Structure by the KL Expansion)

Yasuhiko SAKAI**, Nobuhiko TANAKA*** and Takehiro KUSHIDA**

The simultaneous measurement of the velocities at two points with X-type hot wire probes has been performed in three different downstream regions of a plane jet (the potential core region, the interaction region and the self-preserving region). By applying Karhunen-Loève (KL) expansion in space and time, the structure development of the plane jet is investigated from a viewpoint of both space and frequency. From the downstream variation of the eigenfunctions, it is found that in the early stage of the interaction region the profiles of the first u (streamwise component of velocity fluctuation) and v (cross-streamwise component of velocity fluctuation) mode in the low frequency range become self-similar, but in high frequency range these continue to change until the self-preserving region. The characteristics of coherent structure can be extracted efficiently by the two-point spatial velocity correlation reconstructed from the first mode of KL expansion.

Key Words: Jet, Turbulence, Vortex, Flow Measurements, Spatial Velocity Correlation, Karhunen Loève Expansion, Fourier Transform, Coherent Structure

1. Introduction

The purpose of this study is to clarify the development of a plane jet's coherent structure systematically over the wide range from the nozzle's exit to the sufficient downstream region from a viewpoint of both space and frequency. We applied the Karhunen Loève (KL) expansion[1),(2)] which is also referred to as the Proper Orthogonal Decomposition (POD) to extract objectively the coherent structure in the turbulent field. In our previous paper[3)], we performed the simultaneous measurements at two points with the X-type hot wire probes in three regions of a turbulent plane jet (the potential core region, the interaction region and the self-preserving region) and reported the development of the two-point spatial velocity correlations, eigenvalues and eigenfunctions obtained by the KL expansion. In this paper, further by applying the Fourier transform to the temporal axis, the mechanism of structure development of a plane jet is investigated from a viewpoint of frequency in addition to space.

* Received 2nd June, 2006 (No. 04-0809). Japanese Original: Trans. Jpn. Soc. Mech. Eng., Vol.71, No.708, B(2005), pp.1978–1985 (Received 14th July, 2004)

** Department of Mechanical Science and Engineering, Nagoya University, Furo-cho, Chikusa-ku, Nagoya 464–8603, Japan. E-mail: ysakai@mech.nagoya-u.ac.jp

*** Mitsubishi Heavy Industries, Ltd., 1–1, Akunoura-machi, Nagasaki 850–8610, Japan

2. The KL Expansion in Space and Time

In the case of the inhomogeneous and stationary flow field, the KL expansion can be applied in the inhomogeneous direction and the Fourier transform in the temporal axis[4)–9)]. In our previous paper[3)], the KL expansion is applied only to the the vertical (cross-streamwise) direction, i.e., x_2-direction (see Fig. 1). In this paper, the Fourier transform is further applied to the temporal axis τ, and we investigate the turbulent structure from a viewpoint of both space and frequency.

When the eigenfunctions obtained by this analysis are expressed as $\psi_{F\alpha}^{(n)}(x_2,\tau)$ (where α denotes either u or v; u is the axial (x_1-directional) velocity and v is the vertical (x_2-directional) velocity, and τ is the time difference.), $\psi_{F\alpha}$ is given as the solution of the following Fredholm integral eigenvalue equation[4)] whose kernel is the two-point velocity cross-correlation function of velocity $R_{\alpha\alpha}$

$$\int_1 R_{\alpha\alpha}(x_2,x_2',\tau)\psi_{F\alpha}^{(n)}(x_2',\tau)\,\mathrm{d}x_2' = \hat{\lambda}_{F\alpha}^{(n)}(\tau)\psi_{F\alpha}^{(n)}(x_2,\tau), \tag{1}$$

$$R_{\alpha\alpha}(x_2,x_2',\tau) = \langle \alpha(x_2,t)\alpha(x_2',t-\tau)\rangle, \tag{2}$$

where the superscript n denotes the mode number, $\hat{\lambda}_{F\alpha}^{(n)}(\tau)$

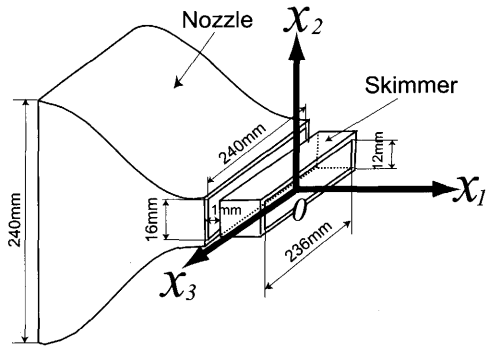

Fig. 1 The skematic of the experimental appartus near the nozzle exit and the coordinate system

is the eigenvalue of the nth mode and $\langle\cdot\rangle$ denotes the ensemble average. A summation convention is not applied to the subscript α, and I is a domain for applying the KL expansion. Now we describe the Fourier transform of $R_{\alpha\alpha}$, $\psi_{F\alpha}^{(n)}$ and $\hat{\lambda}_{F\alpha}^{(n)}$ as $\Phi_{\alpha\alpha}$, $\phi_{F\alpha}^{(n)}$ and $\lambda_{F\alpha}^{(n)}$, respectively. For instance, the Fourier transform of the two-point velocity correlation function $R_{\alpha\alpha}(x_2, x_2', \tau)$ becomes the cross spectrum as follows,

$$\Phi_{\alpha\alpha}(x_2, x_2', f) = \int R_{\alpha\alpha}(x_2, x_2', \tau) e^{-i2\pi f\tau}\, \mathrm{d}\tau. \tag{3}$$

By using the same relations as Eq. (3) between $\psi_{F\alpha}^{(n)}$ and $\phi_{F\alpha}^{(n)}$, $\hat{\lambda}_{F\alpha}^{(n)}$ and $\lambda_{F\alpha}^{(n)}$, we obtain the following transformed equation of Eq. (1),

$$\int_{\mathrm{I}} \Phi_{\alpha\alpha}(x_2, x_2', f)\phi_{F\alpha}^{(n)}(x_2', f)\, \mathrm{d}x_2' = \lambda_{F\alpha}^{(n)}(f)\phi_{F\alpha}^{(n)}(x_2, f). \tag{4}$$

Since the velocity measurements are performed at the discrete spatial points, Eq. (4) leads to the eigenvalue ploblem of the tensor $\Phi_{\alpha\alpha}$ whose eigenvalues and eigenfunctions are $\lambda_{F\alpha}^{(n)}$ and $\phi_{F\alpha}^{(n)}$, respectively. Here, $\Phi_{\alpha\alpha}$ is a complex number, so we have to solve the complex number eigenvalue ploblem. But in the present case, the eigenvalues $\lambda_{F\alpha}^{(n)}(f)$ are positive real numbers and the eigenfunctions $\phi_{F\alpha}^{(n)}(x_2, f)$ are complex numbers because $\Phi_{\alpha\alpha}$ is Hermitian[6].

The important properties of the KL expansion in space and time are explained as follows (see Refs. (4)–(6) for the details).

(a) The eigenvalues are arranged in order of magnitude

$$\lambda_{F\alpha}^{(1)}(f) > \lambda_{F\alpha}^{(2)}(f) > \cdots > \lambda_{F\alpha}^{(n)}(f) \tag{5}$$

(b) The Fourier transform of the velocity field $\hat{\alpha}(x_2, f)$ can be expressed as a linear combination of the eigenfunctions

$$\hat{\alpha}(x_2, f) = \sum_{n=1}^{\infty} a_{F\alpha}^{(n)}(f)\phi_{F\alpha}^{(n)}(x_2, f), \tag{6}$$

where the random coefficients $a_u^{(n)}(f)$ are given by,

$$a_{F\alpha}^{(n)}(f) = \int_{\mathrm{I}} \alpha(x_2, f)\phi_{F\alpha}^{(n)}(x_2, f)\, \mathrm{d}x_2. \tag{7}$$

(c) The mean square value of the fluctuating velocity integrated over the domain I is given by the sum of the eigenvalues integrated over all frequency range,

$$E_\alpha = \int_{\mathrm{I}} \left\langle \alpha^2(x_2) \right\rangle \mathrm{d}x_2 = \sum_n \int_f \lambda_{F\alpha}^{(n)}(f)\, \mathrm{d}f. \tag{8}$$

(d) The cross spectrum $\Phi_{\alpha\alpha}$ and the power spectrum S_α are reconstructed by the following equations

$$\Phi_{\alpha\alpha}(x_2, x_2', f) = \sum_{n=1}^{\infty} \lambda_{F\alpha}^{(n)}(f)\phi_{F\alpha}^{(n)}(x_2, f)\phi_{F\alpha}^{(n)*}(x_2', f), \tag{9}$$

$$S_\alpha(x_2, f) = \sum_{n=1}^{\infty} \lambda_{F\alpha}^{(n)}(f)|\phi_{F\alpha}^{(n)}(x_2, f)|^2, \tag{10}$$

where $*$ denotes a complex conjugate.

3. Experimental Methods and Conditions

The experimental methods and conditions are the same as our previous work[3], so we briefly explain them in this paper. Figure 1 shows the schematic of the experimental apparatus near the nozzle exit and the coordinate system. The skimmer was installed at the position of about 1 mm downstream from the nozzle exit to eliminate the boundary layer which develops along the contraction wall. The height d and the width l of the skimmer exit are 12 mm and 236 mm, respectively (the aspect ratio of the skimmer exit is 19.7). In this study, the velocity U_0 at the skimmer exit is about 20 m/s, so Reynolds number $Re(= U_0 d/\nu)$ is about 16 000. The coordinate system is as follows: the axial (streamwise) coordinate is x_1, the vertical (cross-streamwise) coordinate is x_2 and the spanwise coordinate is x_3.

The flow field of a plane jet is divided broadly into the potential core region, the interaction region and the self-preserving region from the skimmer's exit toward the downstream. It is practically difficult to determine the boundary between these regions because the actual flow field continuously develops. It is very difficult and arbitrary to determine the start of the self-preserving region. In this study, we define that the self-preserving region as a region with a similarity with respect to the vertical (x_2) profile of both the mean velocity and the r.m.s. velocity, and then experimentally distinguished three regions. In our previous paper[3], the velocity measurements were carried out with a signal X-type hot-wire probe and the fundamental properties of the present plane jet were examined. From these results, it was found that the mean velocity shows a good similarity at $x_1/d > 5.0$ and the r.m.s. velocity shows a good similarity at $x_1/d > 10.0$. Therefore, as the measurement locations for the present KL expansion, six downstream locations were chosen, i.e., $x_1/d = 2.0, 3.0$ (in the potential core region), $x_1/d = 4.5$ (in the early stage of the interaction region), $x_1/d = 6.0$ (in the late stage of the interaction region) and $x_1/d = 10.0, 20.0$ (in the self-preserving region).

In this study, the cross spectrum is obtained not by the Fourier transform of the cross-correlation function, but by the fast Fourier transform (FFT) of the time series of discrete and finite data. The Nyquist frequency (the recoverable maximum frequency) is 5 kHz because the present experimental sampling frequency is 10 kHz. The frequency resolution is $1/2^{11}$ (= 1/2 048) of the Nyquist frequency from the restriction of FFT, i.e., about 2.4 Hz. Therefore, we solve 2 047 eigenvalue problems of 21×21 cross spectrum tensor (the eigenvalue for $f = 0.0$ Hz can not be calculated).

4. Results of Analysis

4.1 Eigenvalues

4.1.1 Energy contributions Tables 1 and 2 show energy contributions from the 1st to the 5th mode for the velocity components u and v. The energy contribution is defined as the ratio of the integral value of each eigenvalue over all frequency range ($\int_f \lambda_{F\alpha}^{(n)}(f)\,\mathrm{d}f$) to the sum of these integral values over all modes ($\sum_{n=1}^{21} \int_f \lambda_{F\alpha}^{(n)}(f)\,\mathrm{d}f$), and it is expressed by the percentage (%). From these tables, it is found that there is a big difference between the energy distributions in the potential core region ($x_1/d = 2.0, 3.0$) and in the downstream of the interaction region ($x_1/d = 4.5 \sim 20.0$). In the potential core region, the contribution of the 1st mode is about 50% for both u- and v-component. This means only one mode achieves half of all fluctuation energy. On the contrary, the contribution of the 1st mode decreases to about 30% in the downstream of the interaction region. The characteristic like this agrees with the results of other researchers[5),(6)].

4.1.2 Eigenspectra Figures 2 (a) and (b) show the downstream variations of the eigenspectra for the 1st u,v-mode $\lambda_{Fu}^{(1)}(f)$ and $\lambda_{Fv}^{(1)}(f)$, where each of eigenspectra is normalized by the sum of frequency integrals of eigenspectra over all modes ($\lambda_{F\alpha,total} = \sum_{n=1}^{21} \int_f \lambda_{F\alpha}^{(n)}(f)\,\mathrm{d}f$). Although the figure is not shown here, it is ascertained that the downstream variations of $\lambda_{Fu}^{(1)}(f)$ and $\lambda_{Fv}^{(1)}(f)$ are very similar to the downstream variations of the ordinary power spectra of the fluctuating velocity components. We notice that $\lambda_{F\alpha}^{(n)}(f)$ essentially has the similar meaning to the power spectrum since the spatial integral of the mean square value of the fluctuating velocity is given by the sum of the frequency integrals of eigenvalues (Eq. (8)). So $\lambda_{F\alpha}^{(n)}(f)$ is commonly called by "eigenspectrum". But, it should be noted that the eigenspectrum is not completely the same as the power spectrum. The reason is that the eigenspectrum varies with the number of mode n. In particular, the first mode ($n = 1$) is important, and it is usually used to extract the most energetic (generally the large scale) structure. However, from Figs. 2 (a) and (b), the $-5/3$ power law can be observed at $x_1/d = 20.0$. This means that the first mode can also contain the small scale structure with the local isotropy in the high frequency range (probably in the inertial subrange). As described in section 4.2, this seems to be related with the fact that the shape of the first u-mode agrees with the one of the first v-mode in high frequency range. Further, although it is not shown here, we confirmed that the ordinary power

Table 1 Percentage of fluctuation energy in the first five u-eigenvalues of the KL expansion (%)

x_1/d	2.0	3.0	4.5	6.0	10.0	20.0
1st mode	43.7	55.6	29.6	31.2	27.5	33.3
2nd mode	27.6	23.3	20.4	22.9	21.2	22.8
3rd mode	11.2	9.25	12.1	11.6	11.6	12.8
4th mode	8.1	4.34	9.8	9.1	9.8	9.5
5th mode	4.2	2.77	7.9	6.4	7.4	6.4

Table 2 Percentage of fluctuation energy in the first five v-eigenvalues of the KL expansion (%)

x_1/d	2.0	3.0	4.5	6.0	10.0	20.0
1st mode	52.5	60.0	33.7	35.6	36.4	33.3
2nd mode	32.5	31.4	15.6	15.5	16.3	13.6
3rd mode	5.8	3.2	12.0	10.1	10.2	10.7
4th mode	3.7	2.1	9.7	8.0	8.5	8.6
5th mode	2.3	1.4	7.5	6.7	6.7	7.2

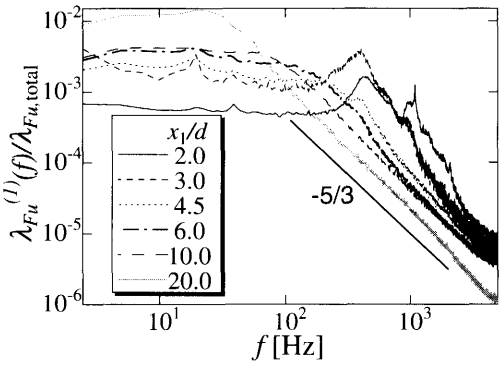

(a) First u-eigenspectra

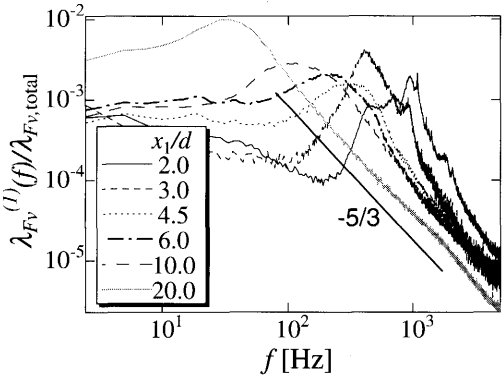

(b) First v-eigenspectra

Fig. 2 The downstream variations of the first u- and v-eigenspectrum

spectrum of v at the same location shows -1.4 power law. The value -1.4 is consistent with Sreenivasan's estimation[10], which shows that the slope of the power spectrum of v is about -1.4 at $R_{\lambda_g} \sim 400$ (which corresponds to the turbulent Reynolds number based on the Taylor transverse micro scale λ_g at $x_1/d = 20.0$ in this plane jet). Therefore it is found that the eigenspectrum of the first v-mode shows the slope nearer to $-5/3$ in comparison with the slope of the ordinary power spectrum.

4.2 Eigenfunctions (modes)

Figures 3 (a) – (e) and 4 (a) – (e) show the downstream variations of the 1st u and v modes, respectively. The abscissas are x_2 normalized by the half width b and f, and the ordinate is the absolute value of the eigenfunction $\phi^{(1)}_{Fa}(x_2, f)$ because it is a complex number. As it goes downstream, the profiles of eigenfunctions $\phi^{(1)}_{Fu}$ and $\phi^{(1)}_{Fv}$ changes gradually, but in the self-preserving region ($x_1/d = 10.0, 20.0$, Figs. 3 (d) and (e), Figs. 4 (d) and (e)) they keep almost the same shape. Further, seeing the low frequency range, we find that at the early stage of the interaction region ($x_1/d = 4.5$) the profile has already shown almost the same shape as the one in the self-preserving region. On the contrary, in high frequency range the profile continues to change until the self-preserving region. This means that the low frequency structure, i.e., the large scale structure is first formed and then the high frequency structure (the small scale structure) is formed. Consequently, it is considered that this expresses the energy transfer process between wavenumbers in the development of the jet structure.

Now, we consider the shape's change of the eigenfunction in more detail. In the potential core region ($x_1/d = 2.0$), the 1st u-mode (Fig. 3 (a)) shows zero near the jet centerline ($x_2/b \approx 0$) and the peaks at both sides of the jet centerline over all frequency range. These two peaks are caused by the vortex structure formed in the shear mixing layer between the stationary fluid in the outside of the potential core and the fluid ejected from the skimmer exit. In contrast, the 1st v-mode (Fig. 4 (a)) has the peaks at both sides in high frequency range like the first u-mode, but in the low frequency range one-side peak at only $x_2/b > 0$. Although it is not shown here, we find that the 2nd u-mode has one-side peak at only $x_2/b < 0$ in the low frequency range. So the summation of the 1st and 2nd v-mode leads to the symmetric shape about the jet centerline in the low frequency range. Further, it is found that at the downstream of the interaction region the 1st u-mode keeps two peaks and the 1st v-mode keeps one peak in low frequency range. These results agree with the characteristics of the 1st mode in the self-preserving region reported by Gordeyev and Thomas[6].

Seeing the high frequency range, we find that for both u- and v-mode the value near the jet centerline increases as

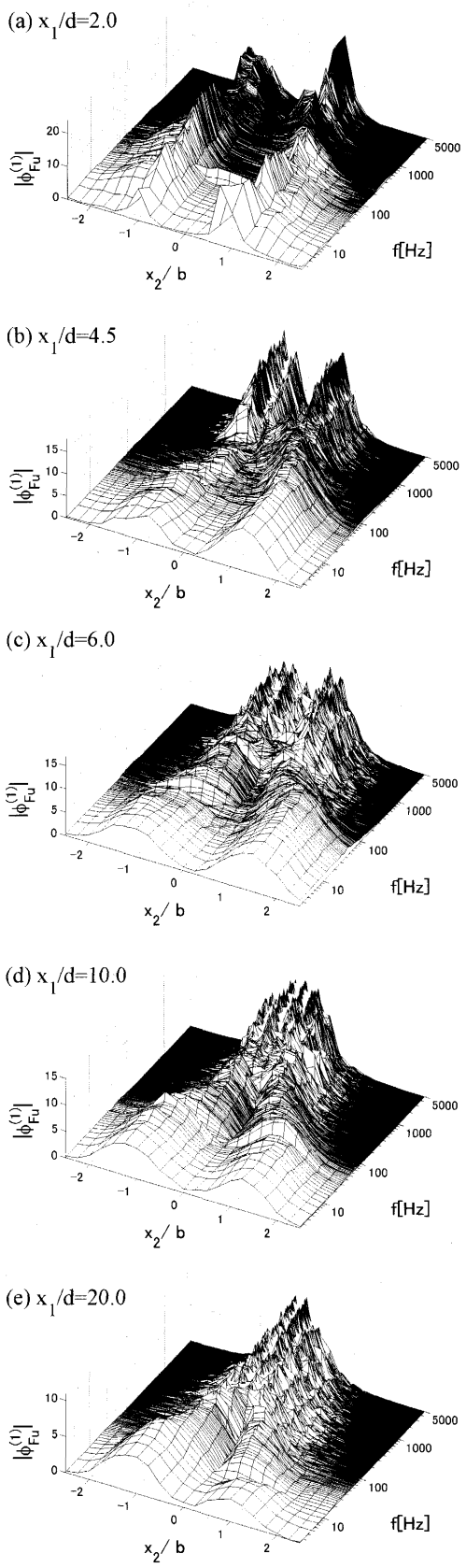

Fig. 3 The downstream variation of the first u-mode

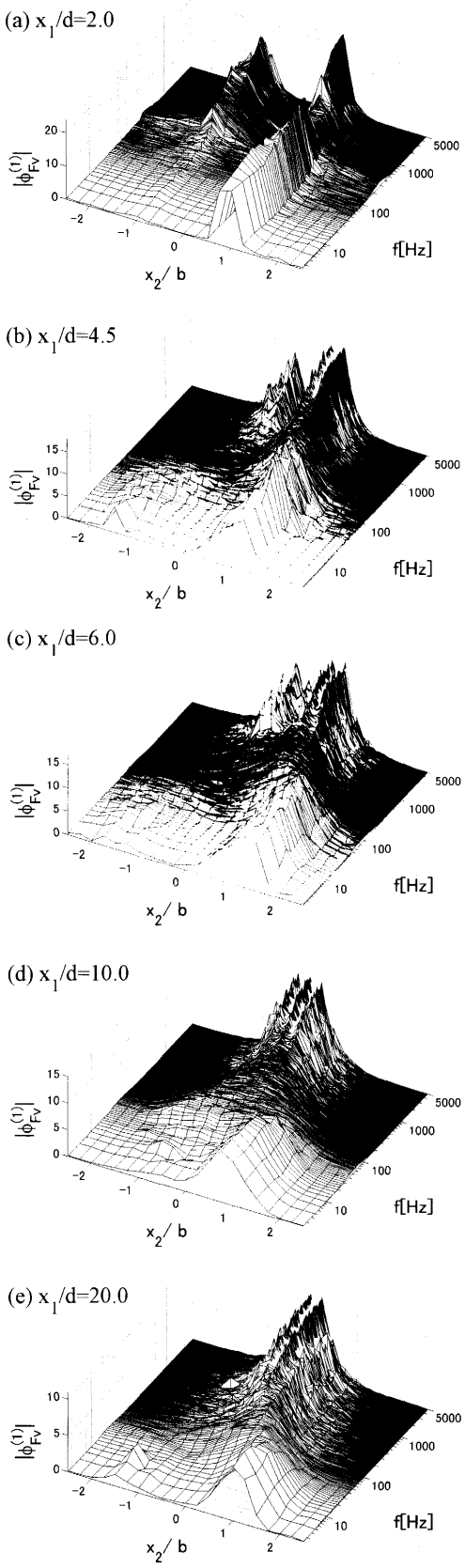

Fig. 4 The downstream variation of the first v-mode

it goes downstream, and then in the self-preserving region ($x_1/d = 10.0$) two peaks at both sides disappear, whereas one peak grows around the jet centerline. The shapes of u- and v-mode in the high frequency range are similar with each other. This suggests that the small scale structure has the isotropic character.

4.3 Reconstruction of two-point spatial velocity correlations

Figures 5 (a) – (d), 6 (a) – (d) and 7 (a) – (d) show the original and reconstructed u- and v- spatial correlation at $x_1/d = 2.0, 4.5, 20.0$, respectively. The reconstruction of the two-point correlation function is made as follows. From Eq. (9), we firstly calculate the reconstructed cross spectrum, and then the reconstructed two-point velocity cross-correlation function can be obtained by the inverse Fourier transform,

$$R^{(1)}_{\alpha\alpha}(x_2, x_2', \tau) = \int_{-\infty}^{\infty} \Phi^{(1)}_{\alpha\alpha}(x_2, x_2', f) e^{i2\pi f\tau} \mathrm{d}f. \qquad (11)$$

From Eq. (11), we notice that the value of the cross-correlation function $R^{(1)}_{\alpha\alpha}(x_2, x_2', 0)$ for $\tau = 0$ becomes an usual two-point spatial velocity correlation. The reconstructed two-point spatial velocity correlation $C^{(1)}_{\alpha\alpha}(x_2, x_2')$ is obtained by calculating for all x_2 and x_2' positions.

$$C^{(1)}_{\alpha\alpha}(x_2, x_2') = \frac{R^{(1)}_{\alpha\alpha}(x_2, x_2', 0)}{\sqrt{\langle \alpha^{(1)}(x_2, t)^2 \rangle} \sqrt{\langle \alpha^{(1)}(x_2', t)^2 \rangle}}. \qquad (12)$$

Further, the original two-point spatial velocity correlation is caluculated by the following equation,

$$C_{\alpha\alpha}(x_2, x_2') = \frac{\langle \alpha(x_2, t)\alpha(x_2', t) \rangle}{\sqrt{\langle \alpha(x_2, t)^2 \rangle} \sqrt{\langle \alpha(x_2', t)^2 \rangle}}, \qquad (13)$$

where α denotes u or v, and the value of $C_{\alpha\alpha}$ is in the range $[-1.0, +1.0]$. From these figures it is found that the reconstructed distributions show more complex shape with the steeper gradients in comparison with the original one. It is known that in the self-preserving region the original u-correlation $C_{uu}(x_2, x_2')$ is negative at the symmetric positions with respect to the jet centerline (i.e., at the second and fourth quadrant in the figure)[11]–[13], and this is one of the important features of the coherent structure in a plane jet. In this study, from Fig. 7 (a) it is also found that the distribution of the original u-correlation in the self-preserving region ($x_1/d = 20$) shows the negative lobes whose values are about -0.1 at the second and fourth quadrant. In contrast, the u-correlation reconstructed by the 1st mode $C^{(1)}_{uu}$ (Fig. 7 (b)) shows the clearer and larger lobes whose values are about -0.4. Thus, the original correlation shows the smaller negative value than the one of the reconstructed correlation by the first mode. This means that the KL expansion can remove the influence of the small scale turbulence on the correlation to some extent and extract the coherent structure efficiently. The reason why the KL expansion can extract the coherent

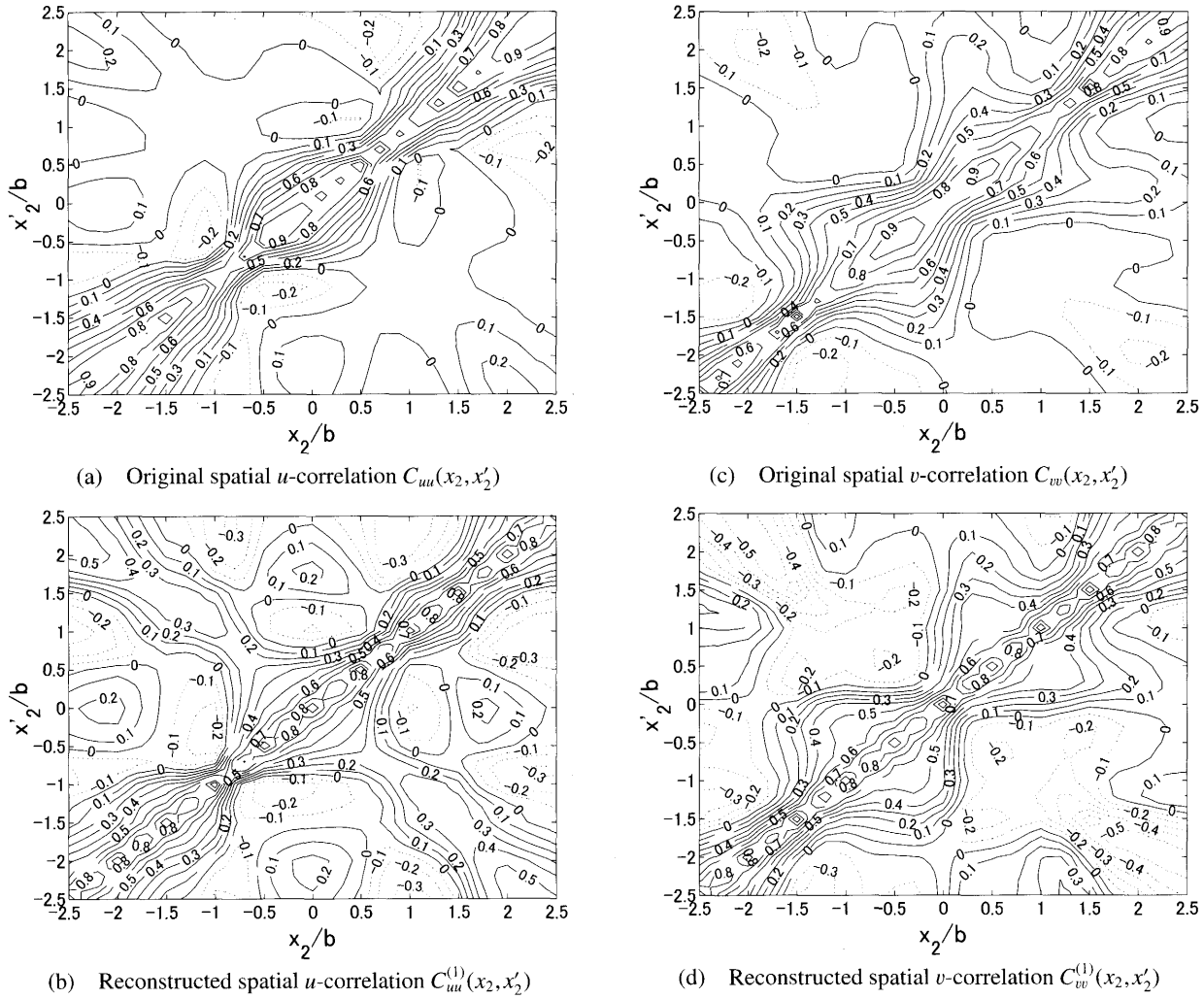

(a) Original spatial u-correlation $C_{uu}(x_2, x_2')$

(c) Original spatial v-correlation $C_{vv}(x_2, x_2')$

(b) Reconstructed spatial u-correlation $C_{uu}^{(1)}(x_2, x_2')$

(d) Reconstructed spatial v-correlation $C_{vv}^{(1)}(x_2, x_2')$

Fig. 5 Original and reconstructed spatial u- and v-correlation in the potential core region $(x_1/d = 2.0)$

structure is that the KL expansion is originally an analysis based on the spatial correlation. The small scale turbulence has generally a weak spatial correlation, whereas the coherent structure has a strong spatial correlation which can be efficiently extracted by the KL expansion. Therefore, it can be expected that the reconstructed distributions extract the most characteristic structure in other regions too.

In the potential core region, the reconstructed correlations of u (Fig. 5 (b)) and v (Fig. 5 (d)) show the larger positive and negative values at the symmetric positions with respect to the jet centerline (at the second and fourth quadrant) in comparison with the original correlations (Figs. 5 (a) and (c)), respectively. These characteristics seem to arise from the counter-rotating vortices formed symmetrically with respect to the jet centerline in the potential core region. However, in the interaction region, the values of the reconstructed correlation of u (Fig. 6 (b)) are not so different from the original ones (Fig. 6 (a)). This means that there are no characteristic structures in the interaction region, but it is considered that the symmetric vortices formed in the potential core region have collapsed and the new stable structures are being reconstructed towards the self-preserving region.

5. Conclusions

The simultaneous measurement of the velocities at two points with X-type hot-wire probes has been performed in the different downstream locations of a plane jet, from the skimmer exit to the far downstream self-preserving region. The KL expansion was applied to investigate the structure development of a plane jet from a viewpoint of both space and frequency. For both u (streamwise) and v (cross streamwise) component, the downstream variations of eigenspectra, eigenfunctions and the reconstructed two-point spatial velocity correlations by the 1st mode were examined in detail. The conclusions are summarized as follows

(1) From the investigation of eigenvalues, it is found that the energy contributions of the 1st modes for both ve-

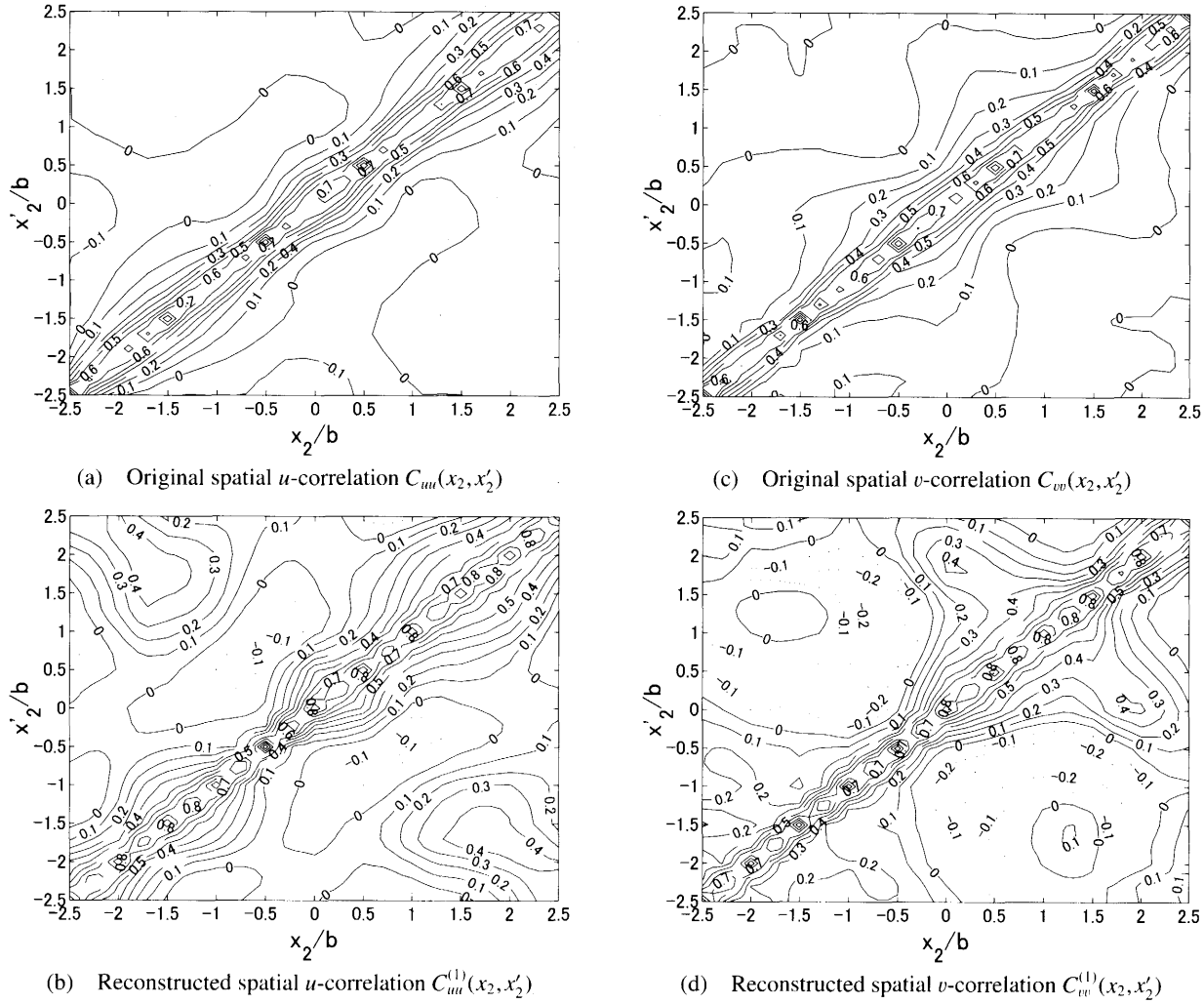

(a) Original spatial u-correlation $C_{uu}(x_2, x_2')$

(c) Original spatial v-correlation $C_{vv}(x_2, x_2')$

(b) Reconstructed spatial u-correlation $C_{uu}^{(1)}(x_2, x_2')$

(d) Reconstructed spatial v-correlation $C_{vv}^{(1)}(x_2, x_2')$

Fig. 6 Original and reconstructed spatial u- and v-correlation in the interaction region ($x_1/d = 4.5$)

locity components u and v are about 50% in the potential core region and decrease to about 30% at the downstream of the interaction region.

(2) The shapes of the eigenfunctions gradually change as it goes downstream. From the downstream variation of the eigenfunctions, it is found that in the early stage of the interaction region ($x_1/d = 4.5$) the shapes of the 1st u- and v-mode in the low frequency range become self-similar, but in high frequency range these continue to change until the self-preserving region ($x_1/d = 10.0$). Further, the shapes of u- and v-mode in high frequency range are similar with each other over the whole downstream regions.

(3) The characteristics of coherent structure can be extracted efficiently by the two-point spatial velocity correlation reconstructed from the 1st mode of the KL expansion. In the potential core and self-preserving region, the reconstructed correlations of both u and v component show the larger values at the symmetric positions about the jet centerline in comparison with the original correlations. On the other hand, in the interaction region, the values of the reconstructed correlation of u are not so different from the original ones. This means that there are no characteristic structures in the interaction region. However it is considered that in the interaction region the symmetric vortices formed in the potential core region have collapsed and the new coherent structures are being reconstructed towards the self-preserving region.

References

(1) Holmes, P., Lumley, J.L. and Berkooz, G., Turbulence, Coherent Structures, Dynamical Systems and Symmetry, (1996), pp.86–128, Cambridge Univ. Press.

(2) Lumley, J.L., The Structure of Inhomogeneous Turbulent Flows, Atmospheric Turbulence and Radio Wave Propagation, Edited by Yaglom, A.M. and Tatarsky, V.I., (1967), pp.166–178, Nauka, Moscow.

(3) Sakai, Y., Tanaka, N. and Kushida, T., On the Development of Coherent Structure in a Plane Jet (Part 1, Characteristics of Two-Point Velocity Correlation and Analysis of Eigenmodes by the KL Expansion), JSME Int. J., Ser.B, Vol.49, No.1 (2006), pp.115–124.

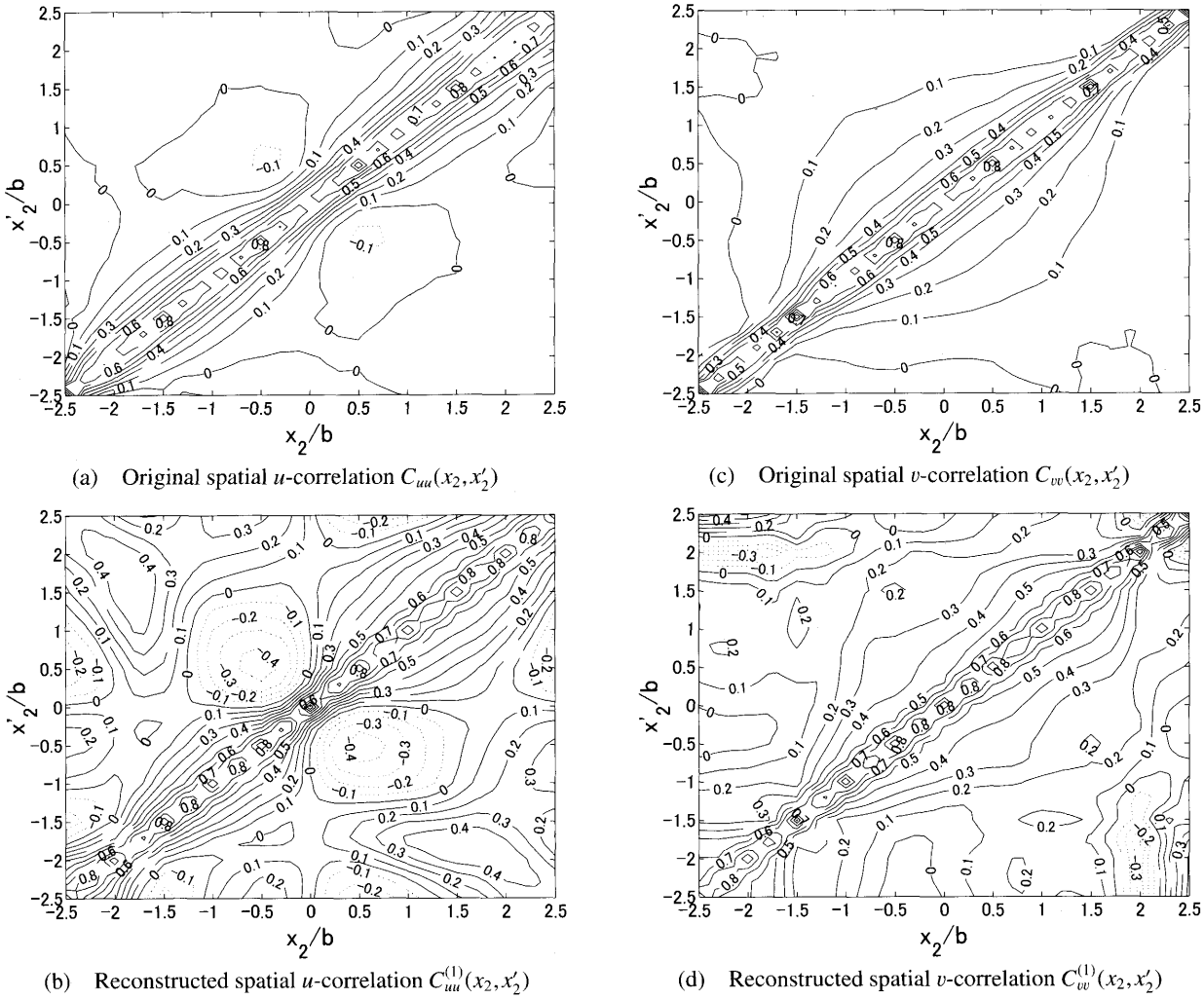

(a) Original spatial u-correlation $C_{uu}(x_2, x_2')$

(c) Original spatial v-correlation $C_{vv}(x_2, x_2')$

(b) Reconstructed spatial u-correlation $C_{uu}^{(1)}(x_2, x_2')$

(d) Reconstructed spatial v-correlation $C_{vv}^{(1)}(x_2, x_2')$

Fig. 7 Original and reconstructed spatial u- and v-correlation in the self-preserving region ($x_1/d = 20.0$)

(4) Delville, J., Bellin, S. and Bonnet, J.P., Use of the Proper Orthogonal Decomposition in a Plane Turbulent Mixing Layer, Turbulence and Coherent Structure, Edited by Metatis, O. and Lesieu, M., (1989), pp.75–90, Kluwer.

(5) Citrinniti, J.H. and George, W.K., Reconstruction of the Global Velocity Field in the Axisymmetric Mixing Layer Utilizing the Proper Orthogonal Decomposition, J. Fluid Mech., Vol.418 (2000), pp.137–166.

(6) Gordeyev, S.V. and Thomas, F.O., Coherent Structure in the Turbulent Planner Jet. Part 1. Extraction of Proper Orthogonal Decomposition Eigenmodes and Their Self-Similarity, J. Fluid Mech., Vol.414 (2000), pp.145–194.

(7) Gordeyev, S.V. and Thomas, F.O., Coherent Structures in the Turbulent Planar Jet. Part 2. Structural Topology via POD Eigenmode Projection, J. Fluid. Mech., Vol.460 (2002), pp.349–380.

(8) Jung, D., Gamard, S. and George, W.K., Downstream Evolution of the Most Energetic Modes in a Turbulent Axisymmetric Jet at High Reynolds Number. Part 1. The Near-Field Region, J. Fluid Mech., Vol.514 (2004), pp.173–204.

(9) Gamarad, S., Jung, D. and George, W., Downstream Evolution of the Most Energetic Modes in a Turbulent Axisymmetric Jet at High Reynolds Number. Part 2. The Far-Field Region, J. Fluid. Mech., Vol.514 (2004), pp.205–230.

(10) Sreenivasan, K.R., The Passive Scalar Spectrum and the Obukhov-Corrsin Constant, Phys. Fluids, Vol.8 (1996), pp.189–196.

(11) Goldschmidt, V.W. and Bradshow, P., Flapping of a Plane Jet, Phys. Fluids, Vol.16, No.3 (1973), pp.354–355.

(12) Cervantes de Gortari, J. and Goldschmidt, V.W., The Apparent Flapping Motion of a Turbulent Plane Jet-Further Experimental Results, J. Fluid Eng., Vol.103 (1981), pp.119–126.

(13) Antonia, R.A., Chambers, A.J., Britz, D. and Browne, L.W.B., Organized Structures in a Turbulent Plane Jet, J. Fluid. Mech., Vol.134 (1983), pp.49–66.